Chinese Chemical Letters 31 (2020) 1398–1401

Contents lists available at ScienceDirect

Chinese Chemical Letters

journal homepage: www.elsevier.com/locate/cclet

Communication

Ferriporphyrin-inspired MOFs as an artificial metalloenzyme for highly sensitive detection of H_2O_2 and glucose

Jiajia Chen, Huajian Gao, Zhihao Li, Yingxue Li, Quan Yuan*

Key Laboratory of Analytical Chemistry for Biology and Medicine (Ministry of Education), College of Chemistry and Molecular Sciences, Wuhan University, Wuhan 430072, China

ARTICLE INFO

Article history:
Received 11 February 2020
Received in revised form 10 March 2020
Accepted 19 March 2020
Available online 20 March 2020

Keywords:
Metalloenzyme
Metal-organic frameworks
Peroxidase
Catalyze
Stability

ABSTRACT

Metalloenzymes which employ metal species and organic ligands as central active sites play significant roles in various biological activities. Development of artificial metalloenzymes can help to understand the related physiological mechanism and promote the applications of metalloenzymes in biosynthesis, energy conversion and biosensing. In this work, inspired by the active sites of ferriporphyrin-based metalloenzymes, Fe-MOFs by using ferric as the metal center and a porphyrin analog as the organic ligand were developed as an artificial metalloenzyme. The Fe-MOFs exhibit high peroxidase-like catalytic activity with excellent long-term stability. Moreover, highly sensitive biosensors were built to detect H_2O_2 and glucose based on the Fe-MOFs. Such MOFs-based artificial metalloenzyme offers an efficient strategy for the development of highly stable and efficient metalloenzymes, showing great potential in catalysis, energy transfer, biosensing and medical diagnosis.

Metalloenzymes are proteins that employ metal ions as the cofactor to regulate the configuration of active sites and further to catalyze specific biochemical reactions [1]. Owing to the unique physical and chemical properties of metal cofactors and organic ligands, metalloenzymes can serve as the carriers of electrons, atoms and functional groups to promote the catalysis process [2,3]. Benefitting from such properties, metalloenzymes have played significant roles in a series of biological activities including electron transfer [3,4], storage and transport of oxygen [5], biosynthesis [6], and sensing of small molecules [7]. However, because of their protein nature, metalloenzymes usually suffer from fatal drawbacks such as easy denaturation, difficult purification and high cost [8–11]. These disadvantages have severely hindered the investigation of their functions and also limited their practical applications. In this regard, construction of artificial metalloenzymes with high stability and high efficiency is of great importance to reveal related biological mechanisms and promote their applications such as biosensing, biosynthesis, diagnosis and disease treatment.

Metal-organic frameworks (MOFs) are a kind of stable functional materials formed by the coordination of metal central and organic ligands [12]. The metal central and organic ligands endow MOFs with various characteristics including catalytic, photonic, electronic, and mechanical properties [13–17]. Owing to these outstanding properties, MOFs have received enormous interest in energy harvesting and conversion, biosensing and biomedicine [18–22]. For example, since both the metal central with variable valance and organic ligands with the electron-rich group can serve as electron carriers, MOFs exhibit great advantages in the catalysis of redox reactions [23,24]. More importantly, the framework structures of highly ordered micropores make MOFs with a high specific surface area which provides rich absorption sites and enormous catalytic sites, ensuring the excellent catalytic performance of MOFs [25–27]. In this regard, the similar chemistry nature to metalloenzymes and excellent catalytic properties make MOFs as ideal candidates for artificial metalloenzymes.

Ferriporphyrin is a kind of important molecules in metalloenzymes, playing significant roles in the catalytic properties of peroxidase, heme oxygenase and cytochrome P450 monooxygenase [28–31]. In this work, by using iron ions as the metal central and porphyrin analogs as the organic ligands, a MOFs-based artificial metalloenzyme with peroxidase-like activity was developed (Fe-MOFs). The as-developed Fe-MOFs exhibit highly ordered microporous nanostructure and can provide enormous active sites for absorption and catalysis. Benefitting from such structural properties, Fe-MOFs display excellent peroxidase-like activities. Furthermore, highly sensitive colorimetric biosensors to detect H_2O_2 and glucose were constructed based on Fe-MOFs. Our

* Corresponding author.
E-mail address: yuanquan@whu.edu.cn (Q. Yuan).

https://doi.org/10.1016/j.cclet.2020.03.052

demonstration of MOFs-based artificial metalloenzymes provides an efficient strategy for the construction of bioinspired functional nanomaterials and holds great promise in bioanalysis, disease diagnostics and pollution treatment.

Iron(III)–based metal-organic frameworks (Fe-MOFs) were prepared by a one-step solvothermal reaction with *N,N*-dimethylformamide (DMF) as the solvent. In this reaction, the crystallization of Fe-MOFs is dominated by the coordination of Fe^{3+} and carboxy group in TCPP to promote the nucleation and growth. At the same time, benzoic acid serves as a modulator to regulate the growth and morphology of Fe-MOFs. Transmission electron microscopy (TEM) and scanning electron microscopy (SEM) were utilized to characterize the morphology and structure of the obtained products. As shown in Fig. 1a, the nanoparticles exhibit good monodispersity and a uniform spindle shape with an average size of 185 nm in length and 100 nm in diameter. It is worthy to note that the high-resolution TEM image in Fig. 1b shows that a well-defined lattice fringe and the interplanar spacing is 1.3 nm, corresponding to the micropore diameters of the Fe-MOFs. Such a pore structure is highly ordered and is helpful to improve the specific surface area and provide enormous active sites of Fe-MOFs. SEM image in Fig. 1c further confirms the spindle shape and excellent dispersity of Fe-MOFs. Energy dispersive spectroscopy (EDS) was further used to investigate the elemental composition of Fe-MOFs. The result is presented in Fig. 1d, which indicates that the as-obtained nanoparticles consist of C, Fe, and O elements. All these findings suggest that the Fe-MOFs with highly ordered structure were successfully prepared.

Next, the peroxidase-mimicking activity of Fe-MOFs was investigated by using a chromogenic reaction with 3,3,5,5-tetramethylbenzidine (TMB) as the substrate. As shown in Fig. 2a, on the addition of H_2O_2, the H_2O_2 is decomposed by Fe-MOFs and the simultaneous TMB is oxidized. The oxidized TMB (oxTMB) appeared with blue color and can be measured by UV–vis spectrometer with a maximum absorption peak at 652 nm. As presented in Fig. 2b, when Fe-MOFs were absent, the reaction solution shows no obvious color change and the absorbance variation at 652 nm is negligible. A similar result was observed when H_2O_2 was absent. In contrast, when both Fe-MOFs and H_2O_2 were present in the solution, the reaction solution quickly changes to blue in a few minutes with strong absorbance at 652 nm,

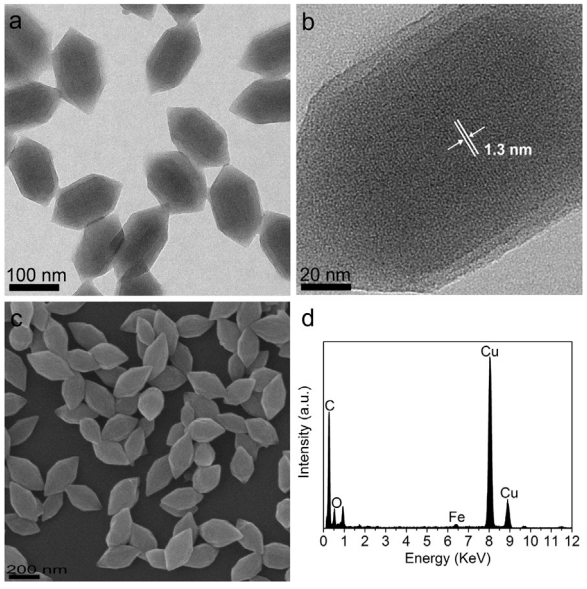

Fig. 1. (a) TEM image of Fe-MOFs. (b) High-resolution TEM image of Fe-MOFs. (c) SEM image of Fe-MOFs. (d) Energy dispersive spectrum of Fe-MOFs. The signal of Cu is from the Cu grid.

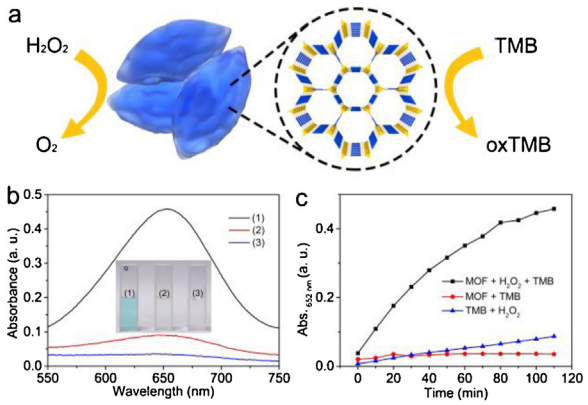

Fig. 2. (a) Schematic illustration for H_2O_2 detection with Fe-MOFs as catalyst. (b) UV–vis spectra of (1) Fe-MOFs, H_2O_2, and TMB, (2) only H_2O_2 and TMB, and (3) only Fe-MOFs and H_2O_2. The inset photograph is the color changes corresponding to the different reaction systems. (c) Time-absorbance curve of different reaction systems. Conditions: Fe-MOFs (30 μg/mL), H_2O_2 (0.1 mmol/L) and TMB (0.05 mmol/L) were incubated in acetate buffer (pH 4.0) at room temperature.

suggesting that the catalytic reaction was carried out only when both Fe-MOFs and H_2O_2 were present. Furthermore, time-dependent response curves of absorption intensity at 652 nm were measured. As shown in Fig. 2c, during the reaction, the solution containing H_2O_2 and TMB remains at the initial absorbance value, and for the solution containing Fe-MOFs and TMB, the absorbance increases slowly. However, the absorption intensity of the solution with Fe-MOFs, H_2O_2 and TMB increases rapidly and then saturates slowly, indicating that the substrate TMB was oxidized. All these findings demonstrate that Fe-MOFs possess peroxidase-like catalytic activity toward TMB oxidation by H_2O_2. According to a previous report [32], we speculated that the possible mechanism is as follows: the O—O bond of the H_2O_2 firstly is broken by the ferriporphyrin analogue on the surface of Fe-MOFs to generate $^{\bullet}OH$, and then TMB is oxidized by the $^{\bullet}OH$.

The peroxidase-like catalytic reaction mechanism was further investigated by a steady-state kinetic model performed with H_2O_2 and TMB as substrates in acetate buffer (50 mmol/L, pH 4.0) at room temperature. For the steady-state kinetic assays, the Michaelis-Menten curve of TMB was obtained by changing TMB

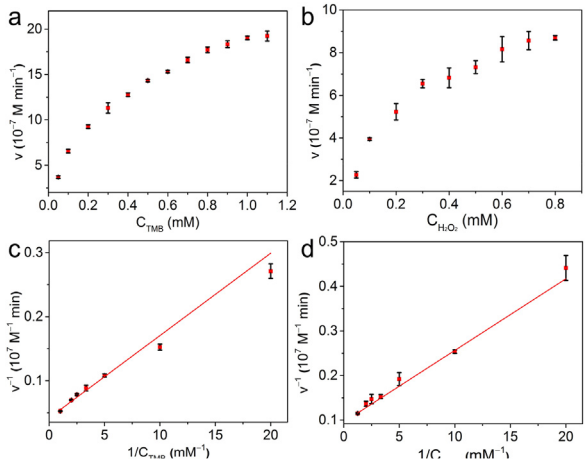

Fig. 3. Steady-state kinetic analysis of Fe-MOFs by using (a, b) Michaelis-Menten model and (c, d) Lineweaver-Burk plots. (a, c) The concentration of TMB was varied from 0.05 mmol/L to 1.10 mmol/L and the concentration of H_2O_2 was fixed at 0.1 mmol/L. (b, d) The concentration of H_2O_2 was varied from 0.05 mmol/L to 0.80 mmol/L and the concentration of TMB was fixed at 0.1 mmol/L. Conditions: Fe-MOFs (30 μg/mL) in acetate buffer (pH 4.0) at room temperature.

concentration and fixing H_2O_2 concentration at 0.1 mmol/L (Fig. 3a). Similarly, the Michaelis-Menten curve of H_2O_2 was obtained by changing H_2O_2 concentration and fixing TMB concentration at 0.1 mmol/L (Fig. 3b). Then, the Michaelis-Menten curves were fitted to the corresponding Lineweaver-Burk plots (Figs. 3c and d). According to the Lineweaver-Burk plots, the kinetic parameters such as maximum initial velocity (V_{max}) and Michaelis-Menten constant (K_m) were obtained to assess the peroxidase-like activity of the Fe-MOFs (Table S1 in Supporting information). Generally, the K_m value is an important indicator for assessing enzyme affinity to its substrates and a lower K_m value represents a higher affinity [33,34]. The K_m value for Fe-MOFs with H_2O_2 as the substrate was 0.17 mmol/L, which was significantly lower than of HRP (3.70 mmol/L). When using TMB as the substrate, the K_m value for Fe-MOFs was 0.31 mmol/L, which was also lower than of HRP (0.43 mmol/L). All these findings suggest that the Fe-MOFs have a higher affinity toward H_2O_2 and TMB than HRP. Furthermore, the V_{max} value of the Fe-MOFs is comparable to HRP with TMB and H_2O_2 as substrates. All these results suggest that Fe-MOFs can be considered as a remarkable peroxidase-like nanozyme.

Owing to its strong oxidizing property and high reactivity, H_2O_2 is prevalent in biological systems as a reactive oxygen species and plays significant roles in cellular signal transduction [35]. The abnormal concentration of H_2O_2 *in vivo* would lead to the imbalance of oxidation environment, and further development of diseases including cancer, neurodegenerative disease, and inflammation [36]. Therefore, the quantitative detection of H_2O_2 plays significant roles in various applications including environmental monitoring, disease diagnosis and mechanism investigation. Based on the peroxidase-like catalytic reaction of the Fe-MOFs, a colorimetric biosensor was designed for the quantitative determination of H_2O_2. Fig. 4a presents the absorbance of the systems with varied H_2O_2 concentrations. It can be clearly observed that the absorbance intensity at 652 nm increases with the H_2O_2 concentration increasing. In addition, Fig. 4b shows a typical response curve between the absorbance at 652 nm and the H_2O_2 concentration. A linear relationship (inset in Fig. 4b) is observed in the range of 0–100 μmol/L with a detection limit of 1.2 μmol/L. Meanwhile, the color changes of the reaction solution can be observed by the naked eye with different concentrations of H_2O_2 (Fig. 4c). All these results indicate that based on the Fe-MOFs, the sensitive biosensors were successfully constructed for H_2O_2 colorimetric detemination.

Glucose is an essential energy source in living cells and plays important roles in the metabolism process of organisms [7,37]. The abnormal glucose concentration is usually a precursor of many diseases such as diabetes, high blood pressure and cancers [37–40].

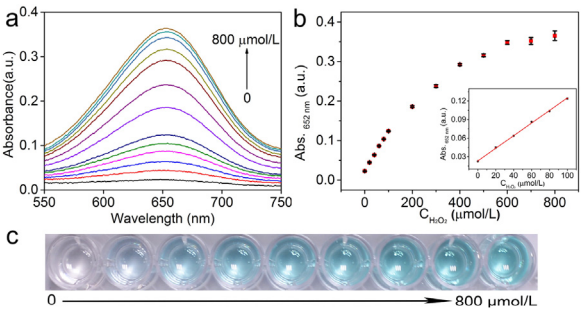

Fig. 4. (a) UV–vis spectra of catalystic systems with Fe-MOFs-based biosensor where the H_2O_2 concentrations were 0, 20, 40, 60, 80, 100, 200, 300, 400, 500, 600, 700 and 800 μmol/L. (b) Absorbance at 652 nm with different H_2O_2 concentration. The inset shows the linear response between the absorbance and H_2O_2 concentration. (c) Corresponding photograph of reaction solutions with different H_2O_2 concentration. Conditions: Fe-MOFs (30 μg/mL) and TMB (0.05 mmol/L) in acetate buffer (pH 4.0) at room temperature.

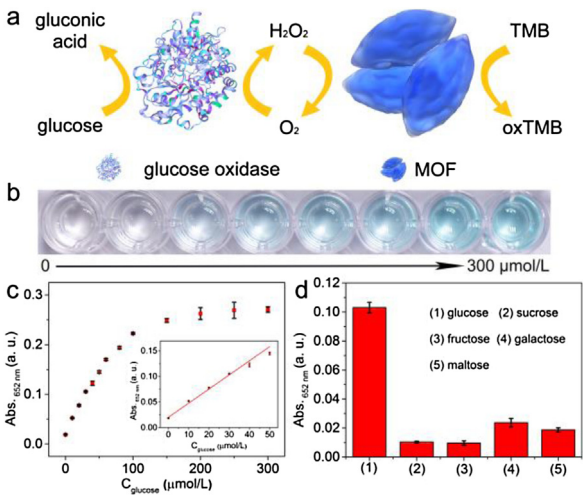

Fig. 5. (a) Schematic illustration of colorimetric detection of glucose with Fe-MOFs-based biosensor. (b) Corresponding photograph of reaction solutions with different glucose concentration. (c) Absorbance at 652 nm with different glucose concentrations. The concentrations of glucose were 0, 10, 20, 30, 40, 50, 60, 80, 100, 200, 300 μmol/L. The insets show the linear response between the absorbance and glucose concentration. (d) Selectivity tests of glucose detection. The concentrations of glucose and glucose analogs are both at 1 mmol/L. Conditions: Fe-MOFs (30 μg/mL) and TMB (0.05 mmol/L) in acetate buffer (pH 4.0) at room temperature.

On the basis of the superior activity toward H_2O_2 of Fe-MOFs, a colorimetric biosensor based on Fe-MOFs was constructed for the quantitative detection of glucose. The scheme for the detection of glucose based on Fe-MOFs is illustrated in Fig. 5a. Glucose is oxidized by glucose oxidase (GOx) in the presence of dissolved oxygen, and at the same time, gluconic acid and H_2O_2 are produced. Subsequently, the formed H_2O_2 is decomposed by Fe-MOFs and simultaneously TMB is oxidized with the generation of a strong absorbance at 652 nm. Photograph of the solutions color as a function of glucose concentrations is shown in Fig. 5b and suggests that the glucose concentration can be easily discriminated by naked eyes. Such visualized detection holds great promise in on-site tests and point-of-care tests. Also, it can be observed from Fig. S6 (Supporting information) that the absorbance intensity of the reaction solution increases gradually with the glucose concentration increasing. Besides, a dynamic range of glucose detection is observed in the concentration from 0 to 300 μmol/L (Fig. 5c). The inset in Fig. 5c further shows that the linear relationship for glucose detection is in the range of 0–50 μmol/L with a detection limit of 0.6 μmol/L, indicating that the biosensors based on Fe-MOFs exhibit excellent sensitivity towards glucose detection. Furthermore, the selectivity of the Fe-MOFs-based biosensor for glucose detection was tested. To conduct the selectivity assays, control experiments were carried out under the same conditions using glucose analogs such as sucrose, fructose, galactose, and maltose. As shown in Fig. 5d, only glucose can generate a significant variation in absorbance. In contrast, there was no significant variation in the absorbance with all of these glucose analogs, which demonstrated that the Fe-MOFs based biosensor shows high selectivity toward glucose. All of our results confirmed that the constructed biosensors exhibited high sensitivity and selectivity for H_2O_2 and glucose colorimetric detection.

In conclusion, an artificial nanozyme with the metalloenzyme-like activity was constructed based on Fe-MOFs. The Fe-MOFs were synthesized based on iron(III) and porphyrin analogs with a similar composition to natural metalloenzymes. The as-prepared Fe-MOFs exhibit highly-ordered micropore structures and display excellent peroxidase-like catalytic activity with high long-term stability. Benefitting from the excellent activity, the artificial nanozyme was utilized to construct highly sensitive and selective colorimetric

biosensors to detect H_2O_2 and glucose, holding great promise in the detection of metabolites. This work opens a new way for the construction of artificial metalloenzyme with high activity and high stability and offers great potentials in biosensing, medical diagnosis and disease therapy.

Declaration of competing interest

The authors declare that they have no known competing financial interests or personal relationships that could have appeared to influence the work reported in this paper.

Acknowledgments

This work was supported by the National Natural Science Foundation of China (Nos. 21925401, 21675120, 21904100) and Changsha Municipal Science and Technology Projects, China (No. kq1901030). Q. Yuan thanks the large-scale instrument and equipment sharing foundation of Wuhan University.

Appendix A. Supplementary data

Supplementary material related to this article can be found, in the online version, at doi:https://doi.org/10.1016/j.cclet.2020.03.052.

References

[1] M. Zhao, H.B. Wang, L.N. Ji, Z.W. Mao, Chem. Soc. Rev. 42 (2013) 8360–8375.
[2] S.H. Lee, D.S. Choi, S.K. Kuk, C.B. Park, Angew. Chem. Int. Ed. 57 (2018) 7958–7985.
[3] V.M. Cangelosi, A. Deb, J.E. Penner-Hahn, V.L. Pecoraro, Angew. Chem. Int. Ed. 53 (2014) 7900–7903.
[4] K. Sadagopan, C. Walgama, Anal. Chem. 85 (2013) 11420–11426.
[5] T. Joshi, B. Graham, L. Spiccia, Acc. Chem. Res. 48 (2015) 2366–2379.
[6] C.N. Jin, S.N. Zhang, Z.J. Zhang, Y. Chen, Inorg. Chem. 57 (2018) 2169–2174.
[7] M. Liu, Z.H. Li, Y.X. Li, J.J. Chen, Q. Yuan, Chin. Chem. Lett. 30 (2019) 1009–1012.
[8] Y.Y. Huang, J.S. Ren, X.G. Qu, Chem. Rev. 119 (2019) 4357–4412.
[9] Z.H. Li, X.D. Yang, Y.B. Yang, et al., Chem. Eur. J. 24 (2018) 409–415.
[10] C. Cui, Q.B. Wang, Q.Y. Liu, et al., Sens. Actuator. B-Chem. 277 (2018) 86–94.
[11] D. Li, B.W. Liu, P.J.J. Huang, Z.J. Zhang, J.W. Liu, Chem. Commun. 54 (2018) 12519.
[12] M.J. van Vleet, T.T. Weng, X.Y. Li, J.R. Schmidt, Chem. Rev. 118 (2018) 3681–3721.
[13] P.Y. Wu, C. He, J. Wang, et al., J. Am. Chem. Soc. 134 (2012) 14991–14999.
[14] J.W. Zhang, H.T. Zhang, Z.Y. Du, et al., Chem. Commun. 50 (2014) 1092–1094.
[15] G. Paille, M. Gomez-Mingot, C. Roch-Marchal, et al., J. Am. Chem. Soc. 140 (2018) 3613–3618.
[16] X. Zhao, B. Pattengale, D. Fan, et al., ACS Energy Lett. 3 (2018) 2520–2526.
[17] C. Hermosa, B.R. Horrocks, J.I. Martínez, et al., Chem. Sci. 6 (2015) 2553–2558.
[18] G. Lan, Y.Y. Zhu, S.S. Veroneau, et al., J. Am. Chem. Soc. 140 (2018) 5326–5329.
[19] M.Q. Wang, Y. Zhang, S.J. Bao, Y.N. Yu, C. Ye, Electrochim. Acta 190 (2016) 365–370.
[20] G.X. Lan, K.Y. Ni, R.Y. Xu, et al., Angew. Chem. 129 (2017) 12270–12274.
[21] X.R. Chen, R.L. Tong, Z.Q. Shi, et al., ACS Appl. Mater. Interfaces 10 (2018) 2328–2337.
[22] Y.F. Li, Z.H. Di, J.H. Gao, et al., J. Am. Chem. Soc. 139 (2017) 13804–13810.
[23] J.W. Liu, Y.Z. Fan, X. Li, et al., Appl. Catal. B: Environ. 231 (2018) 173–181.
[24] Y. Horiuchi, T. Toyao, K. Miyahara, et al., Chem. Commun. 52 (2016) 5190–5193.
[25] X.F. Zhang, L. Chang, Z.J. Yang, et al., Nano Res. 12 (2019) 437–440.
[26] K. Jayaramulu, J. Masa, D.M. Morales, et al., Adv. Sci. 5 (2018) 1801029.
[27] K. Yuan, T.Q. Song, D.W. Wang, et al., Nanoscale 10 (2018) 1591–1597.
[28] X.T. Fan, R.Z. Tian, T.T. Wang, et al., Nanoscale 10 (2018) 22155–22160.
[29] H.J. Cheng, Y.F. Liu, Y.H. Hu, et al., Anal. Chem. 89 (2017) 11552–11559.
[30] F. Nastri, M. Chino, O. Maglio, et al., Chem. Soc. Rev. 45 (2016) 5020–5054.
[31] P.K. Das, S. Samanta, A.B. McQuarters, N. Lehnert, A. Dey, PNAS 113 (2016) 6611–6616.
[32] Y.L. Liu, X.J. Zhao, X.X. Yang, Y.F. Li, Analyst 138 (2013) 4526–4531.
[33] N. Wu, Y.T. Wang, X.Y. Wang, et al., Anal. Chim. Acta 1091 (2019) 69–75.
[34] L.J. Huang, W.X. Zhu, W.T. Zhang, et al., Microchim. Acta 185 (2018) 7.
[35] X. Chen, X. Tian, I. Shin, J. Yoon, Chem. Soc. Rev. 40 (2011) 4783–4804.
[36] G.C. Van de Bittner, C.R. Bertozzi, C.J. Chang, J. Am. Chem. Soc. 135 (2013) 1783–1795.
[37] W.Q. Xu, L. Jiao, H.Y. Yan, et al., ACS Appl. Mater. Interfaces 11 (2019) 22096–22101.
[38] Y.W. Bao, X.W. Hua, H.H. Ran, J. Zeng, F.G. Wu, Chem. B 7 (2019) 296–304.
[39] J.W. Shen, Y.B. Li, H.S. Gu, F. Xia, X.L. Zuo, J. Mater. Chem. Rev. 114 (2014) 7631–7677.
[40] G.B. Mao, Q. Cai, F.B. Wang, et al., Anal. Chem. 89 (2017) 11628–11635.